

Collective phonon excitation in KTaO_3

Akitoshi Koreeda, Ryuta Takano, Akira Ushio, and Seishiro Saikan
Department of Physics, Graduate School of Science, Tohoku University, Sendai 980-8578, Japan
 (Received 4 June 2010; published 3 September 2010)

The collective excitation of phonons, including thermal diffusion and second sound (temperature wave), in KTaO_3 has been studied by low-frequency light-scattering and by time-domain light-scattering techniques. The observed spectra are analyzed with the new spectral formula, which is applicable consistently from hydrodynamic to ballistic (collisionless) phonon regimes. Our analysis of the quasielastic scattering and the anomalous soundlike peak (broad doublet) determines the temperature dependences of the phonon relaxation times for both the normal and resistive processes of the phonon-phonon scattering. It is shown that the normal process is anomalously enhanced at low temperatures as theoretically predicted, and the “frequency window” for the propagating second sound is defined approximately below 30 K.

DOI: [10.1103/PhysRevB.82.125103](https://doi.org/10.1103/PhysRevB.82.125103)

PACS number(s): 63.20.-e, 05.70.Ln, 77.84.Ek, 66.70.-f

I. INTRODUCTION

KTaO_3 is a quantum paraelectric (QPE) in which relatively large zero-point motion is thought to disturb the ferroelectric phase transition.¹ In QPEs, the frequency of a long-wavelength polar optic-phonon mode (soft mode) decreases on cooling but never freezes even at $T=0$ K (Ref. 2). It is thought that the existence of such a low-frequency optical phonon substantially enhances the phonon-phonon collisions against the acoustic-phonon branches, resulting in the anomalously large population of long-wavelength phonons.³ In SrTiO_3 , Hehlen *et al.*⁴ have found an anomalous light-scattering component, which behaved just like the Brillouin scattering from a propagating “sound wave” having a slightly slower velocity than ordinary elastic waves such as the longitudinal and transverse acoustic modes. They proposed that the new soundlike mode be arising from the wavelike propagation of entropy, which is often referred to as the “second sound,”^{5,6} according to the prediction made by Gurevich and Tagantsev.³ However, a number of negative reports have been published from many authors,^{7–11} and its origin has been controversial for a long time. Recently, however, a new measurement and analyzing method that eliminate the ambiguity in the previous analyses have been reported,^{12,13} and the existence of the gigahertz second sound in SrTiO_3 has been found to be very likely. Since similar spectrum has been reported also in KTaO_3 ,^{4,14–16} it is of great interest to investigate such an excitation in this material. The second sound in QPEs such as SrTiO_3 and KTaO_3 is of great importance because these materials are closely related to other interesting phenomena such as superconductivity, ferroelectricity, or quantum fluctuations. If coherent generation of second sound in 10 GHz range is realized, it will be possible to drastically modulate other excited states resident in QPEs.

According to the phonon-transport theory,¹⁷ the most important parameters that characterize the collective excitation of phonons such as thermal diffusion or second sound in crystals are the relaxation times for the normal and resistive scattering processes, denoted as τ_N and τ_R , respectively. In the normal process, the quasimomentum of phonons participating in the anharmonic collision (such as three-phonon or

four-phonon processes) is conserved, whereas it is not in the resistive process, which includes the umklapp process, scattering by impurity, etc. While τ_R can be estimated from the measurement of thermal conductivity or thermal diffusivity, τ_N cannot be known from such measurements.¹⁸ However, it is known that the light-scattering spectra in the Rayleigh-Brillouin range (1–100 GHz frequency) clearly reflects the dynamics of the collective excitation of phonons in crystals,¹⁹ and therefore, the low frequency light scattering is a powerful tool to investigate the temperature dependences of both τ_N and τ_R . For that purpose, we have recently derived¹³ the nonequilibrium dynamic form factor, which can be fitted to the experimental spectra in any phonon regime, i.e., consistently from the hydrodynamic regime (including thermal diffusion and second-sound regime) to the ballistic regimes.

In this paper, we present the temperature dependences of the phonon scattering rates, τ_R^{-1} and τ_N^{-1} , for the resistive and normal processes in KTaO_3 , measured from the low-frequency light-scattering experiments. We first estimate τ_R solely from the time-domain light-scattering measurement,^{20,21} and then analyze the frequency-domain light-scattering spectrum to extract the contribution from the normal processes. The temperature dependences of τ_R and τ_N obtained show that the “frequency window” for the propagating second sound is well defined. Although the present experimental geometry (backscattering) does not allow for a well-defined second sound, our results suggest that it would be possible to observe or generate a better defined second sound in KTaO_3 with the use of much smaller scattering angles.

II. EXPERIMENT

To clarify the temperature dependences of both τ_R and τ_N , we first performed the impulsive stimulated thermal scattering (ISTS) experiment, which enables us to measure the thermal diffusivity in time domain.²⁰ The condition for the second-sound propagation requires that τ_R^{-1} be slower than the natural (bare) frequency of the second sound, which is defined as

$$\omega_0 = \frac{1}{\sqrt{3}}qc, \quad (1)$$

where q and c are the wave-vector transfer and the average sound velocity, respectively. Since the ISTS employs orders of magnitude smaller values of q than those employed in ordinary light-scattering experiments, one can expect that the second sound is heavily overdamped, i.e., $\omega_0 \ll \tau_R^{-1}$, to give almost pure thermal diffusion in the ISTS experiments. The experimental setup for the ISTS was the same as that used in our previous work.²¹ The magnitude of q was varied from 8.27×10^4 to $6.69 \times 10^5 \text{ m}^{-1}$.

The backscattering experiments were, then, performed to obtain the spectrum of the thermal Rayleigh mode,²² broad quasielastic mode,²² and the anomalous “broad doublet” mode.^{15,16,23} The experimental setup is the same as what reported in Ref. 21. The magnitude of q was $5.56 \times 10^7 \text{ m}^{-1}$, which was more than two orders of magnitude larger than those in the ISTS experiments mentioned above.

KTaO₃ is a well-known cubic perovskite-type crystal and does not exhibit any structural phase transition in the temperature range investigated. The sample crystals of KTaO₃ were bulk single crystals. Sample 1 had dimensions of $6 \times 7 \times 8 \text{ mm}^3$, with polished surfaces (110), ($1\bar{1}0$), and (001). Sample 2 had dimensions of $7 \times 8 \times 10 \text{ mm}^3$, with polished surfaces same as Sample 1. The crystal of Sample 1 was made by and purchased from Nippon Telegraph and Telephone Advanced Technology Corporation (NTT-AT) in Japan. Sample 2 was made by MTI Corporation and purchased from NTT-AT. Sample 1 was almost completely colorless and transparent, indicating extremely low density of oxygen vacancies, whereas Sample 2 was less transparent and looked milky probably due to the relatively high density of oxygen vacancies. Each sample was put into a helium-flow-type optical cryostat and the temperature was varied from ~ 6 to 297 K. The direction of q was chosen to be $\parallel[100]$ and $\parallel[110]$.

III. RESULTS

Since the two directions of q ($\parallel[100]$ and $[110]$) gave qualitatively the same results, we present only the results for $q \parallel[100]$ below. Figure 1 shows the typical signals obtained in the ISTS experiment in Sample 1. Note that the vertical axes are in logarithmic scale. Obviously, we see that there are at least two relaxation rates. We also plotted the best-fitted double exponential curves defined as²¹

$$S(t) = A \exp(-2\Gamma_{\text{th}}t) + B \exp(-2\gamma t), \quad (2)$$

where A and B are scaling factors. Γ_{th} is the thermal diffusion rate defined as

$$\Gamma_{\text{th}} = D_{\text{th}}q^2,$$

where D_{th} is the thermal diffusivity. The other relaxation rate, γ , was introduced to reproduce the temporal behavior of the ISTS signal, and its origin was already discussed in Ref. 21, which is out of the main scope of this paper because it is probably not related to phononic phenomenon.

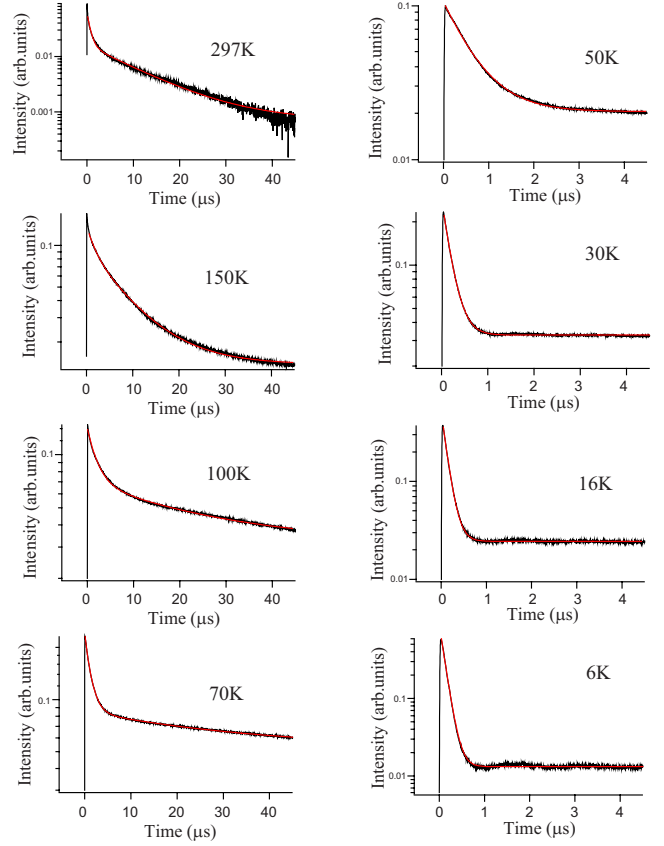


FIG. 1. (Color online) Temperature variation in the signals observed in the ISTS experiment in KTaO₃. The magnitude of q is $1.06 \times 10^5 \text{ m}^{-1}$ and the direction of q is in $[100]$. Note the change in horizontal (time) scale between the left and right sides. The solid lines are the fitted curve expressed by Eq. (2).

It is known that the thermal relaxation rate, Γ_{th} , becomes faster as the temperature is reduced, and that scales as q^2 . We have identified, by changing the magnitude of q , the slower component at 297 K as the thermal relaxation mode, and confirmed that Γ_{th} indeed scales as q^2 as shown in Fig. 2. In contrast, the other relaxation rate, γ , becomes slower on cooling, and was confirmed to be independent of q as shown

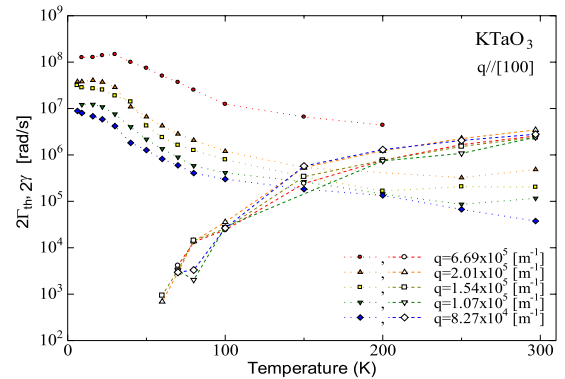


FIG. 2. (Color online) Temperature dependence of $2\Gamma_{\text{th}}$ and 2γ in KTaO₃ (Sample 1). The magnitude of q is varied. The closed and open circles correspond to $2\Gamma_{\text{th}}$ and 2γ , respectively. The values of q for each symbols are shown in the figure.

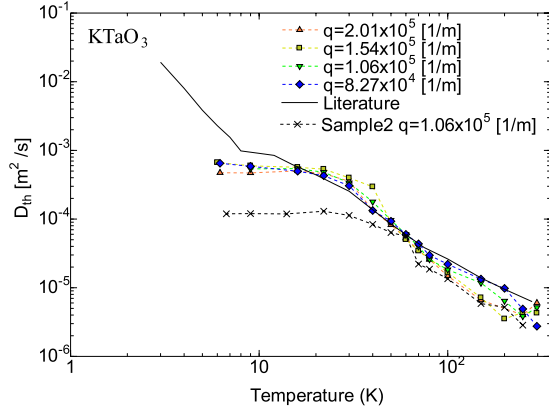


FIG. 3. (Color online) Temperature dependence of the thermal diffusivity of KTaO_3 obtained in this work (symbols) and from literature values (Refs. 24 and 25) (solid line). The values of q for each symbols are shown in the figure.

also in Fig. 2. At relatively low temperatures, γ is sufficiently slow that we could easily separate the two contributions as can be seen in Fig. 1. Although Γ_{th} and γ were difficult to be distinguished between 150 and 200 K, the use of a larger q , viz., $q=6.69 \times 10^5 \text{ m}^{-1}$ enabled us to separate them in this temperature range, and we could determine γ , which is q independent, at all the temperatures investigated. This, in turn, enabled us to determine Γ_{th} at all the temperatures investigated. Since the effective time resolution of our system was approximately 20 ns (50 MHz),²¹ the saturation of Γ_{th} in the low-temperature region of the points for $q=6.69 \times 10^5 \text{ m}^{-1}$, which is the largest q value we employed in this work, is due to the time-resolution limit.

Dividing Γ_{th} by q^2 , we obtain the thermal diffusivity D_{th} ; its temperature dependence is shown in Fig. 3. For comparison, we have also plotted the literature values of the thermal diffusivity derived from the reported values of the thermal conductivity²⁴ and specific heat²⁵ in KTaO_3 , using the following relation:

$$D_{\text{th}} = \frac{\kappa}{\rho C_p},$$

where κ , ρ , and C_p are the thermal conductivity, mass density, and specific heat, respectively. As seen in Fig. 3, the values of D_{th} obtained in this work are in good agreement with those from the literature values at all the temperatures, except for the lowest temperature region approximately below 10 K. The deviation in the low-temperature region is probably due to the strong sample dependence of the thermal conductivity as reported in this material.²⁶ Indeed, Sample 2, which probably contains more oxygen vacancies, exhibited smaller thermal diffusivity than that of Sample 1 as seen in Fig. 3. The resistive relaxation time, τ_{R} , can be estimated from the kinetic expression for D_{th} , viz.,⁵

$$D_{\text{th}} = \frac{1}{3} c^2 \tau_{\text{R}}. \quad (3)$$

In order to estimate the values of τ_{R} from the measured thermal diffusivity by using Eq. (3), it is necessary to determine the average phonon velocity, c . One of the choices of c may be the Debye's average sound velocity, which is calculated to be $\sim 4300 \text{ m/s}$ from acoustic sound velocities estimated from the observed Brillouin shifts. In KTaO_3 , however, the existence of the low-energy optical phonon² must also be considered. Numerical calculation of the second-sound velocity v_{ss} , which is approximately $1/\sqrt{3}$ of c , has been carried out by Farhi *et al.*,^{15,16} considering both the acoustic and optical modes, and they report that $v_{\text{ss}}=1100 \pm 200 \text{ m/s}$. By multiplying $\sqrt{3}$, c can be estimated to be $1900 \pm 350 \text{ m/s}$, which is less than half of the Debye's average sound velocity. Since it turned out that the Debye's velocity yields far worse results in our analysis, we adopted the smaller c value, viz., $c=1900 \text{ m/s}$, in estimating τ_{R} from the relation Eq. (3).

In Fig. 4, we show the frequency-domain light-scattering spectra observed at various temperatures. At high temperatures, there are two quasielastic components:²² the narrower

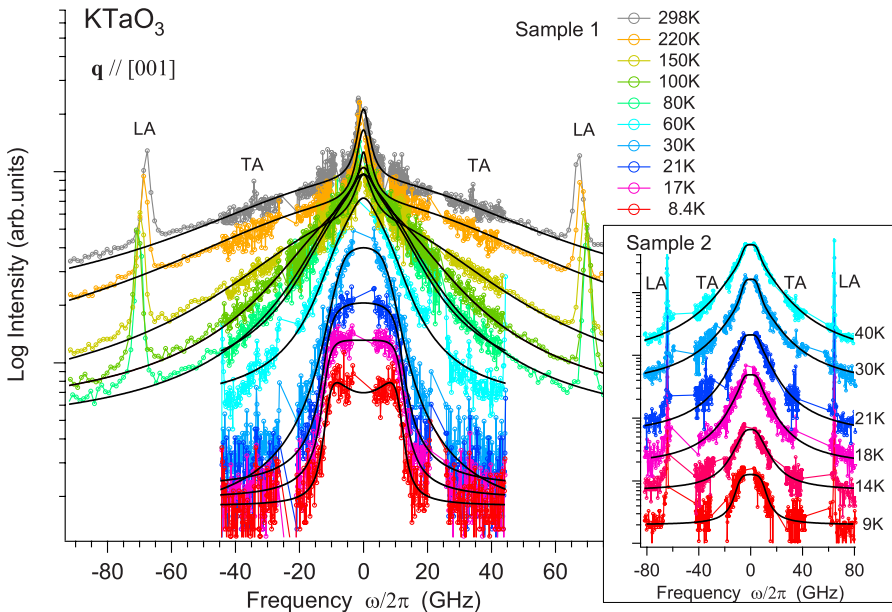


FIG. 4. (Color online) Temperature variation in the back-scattering spectrum observed in KTaO_3 (log-linear plot). The magnitude and direction of q were $5.56 \times 10^7 \text{ m}^{-1}$ and $[001]$, respectively. The solid curves are the fits of Eq. (4). The LA and TA denote longitudinal- and transverse-acoustic modes, respectively. The inset shows the low-temperature spectra observed in Sample 2, which does not exhibit a “doublet” structure.

component due to the thermal diffusion (entropy fluctuations)²² and the broader one due to the nonequilibrium viscosity in the crystal.¹³ The latter component may also be interpreted as arising due to second-order Raman scattering (two-phonon difference scattering) on the same phonon branch.^{13,22} On cooling, the narrower quasielastic component broadens while the broader one narrows:¹³ at around 100 K, the two components are supposed to have almost the same widths. Below 30 K, the narrower quasielastic component in Sample 1 begins to develop into a pair of broad inelastic peaks, which has been reported as the broad doublet by several authors.^{15,16,23} The frequency shift of the broad doublet is approximately 10 GHz, which is about one third of the transverse acoustic frequency (33 GHz). The broad doublet in KTaO₃ does not develop into a well-defined shape as that observed in SrTiO₃.^{4,12,21,23} At the lowest temperature investigated, namely, at 8.4 K, the tail of the spectrum is very steep, despite the fact that the linewidth is broad, which is quite different from what is expected for a usual damped-oscillator spectrum. Actually, such a steep spectral tail is a characteristic of the spectrum in highly nonequilibrium regime as we have demonstrated recently.¹³ In Sample 2, however, the narrow quasielastic component did not develop into a doublet even at the lowest temperature investigated, and the spectral shape remained as a fat unshifted peak.

For the analysis of the spectra, we used the spectral formula recently derived¹³ in terms of extended thermodynamics^{27,28} (ET), which enables us to deal with any phonon regimes covering from hydrodynamic to highly nonequilibrium (collisionless) regimes, owing to the effective inclusion of infinite hierarchy of the moment equations. We have also shown, in Fig. 4, the ET-fitted curves as the solid lines. The formula we fitted is as the following:¹³

$$S_{\text{total}}(q, \omega) = P_1 S_1(q, \omega) + P_2 S_2(q, \omega) + C, \quad (4)$$

where P_1 and P_2 are weighting coefficients, and C is a baseline offset. The component spectra, $S_1(q, \omega)$ and $S_2(q, \omega)$, are defined, respectively, as

$$S_1(q, \omega) = \frac{\omega_0^2 \left(\frac{1}{\tau_R} + \gamma'_3 \right)}{(\omega_0^2 - \omega^2 - \omega \gamma'_3)^2 + \omega^2 \left(\frac{1}{\tau_R} + \gamma'_3 \right)^2}, \quad (5)$$

$$S_2(q, \omega) = \frac{1}{2cq} [\tan^{-1}(\omega + cq)\tau - \tan^{-1}(\omega - cq)\tau], \quad (6)$$

where

$$\frac{1}{\tau} = \frac{1}{\tau_R} + \frac{1}{\tau_N}.$$

$\gamma'_3(q, \omega)$ and $\gamma''_3(q, \omega)$ are, respectively, the real and imaginary parts of the complex memory function, $\gamma_3(q, \omega)$, which is actually an infinitely continued fraction and contains the information on the nonequilibrium dynamics.²⁷ In the present analysis, we approximated the continued fraction by terminating it with the asymptotic form, $\gamma_\infty(q, \omega)$, as²⁹

$$\gamma_3(q, \omega) = \frac{\frac{4}{15}c^2q^2}{i\omega + \frac{1}{\tau} + \gamma_\infty(q, \omega)},$$

which offers an effective inclusion of the whole hierarchy of the moment equation in ET.^{13,27} The real and imaginary parts of $\gamma_3(q, \omega)$ so obtained are written, respectively, as

$$\gamma'_3(q, \omega) = \frac{4}{15}c^2q^2 \times \frac{35}{17} \frac{1/\tau + \frac{18}{17}z'}{\left(\omega + \frac{18}{17}z''\right)^2 + \left(1/\tau + \frac{18}{17}z'\right)^2}, \quad (7)$$

$$\gamma''_3(q, \omega) = -\frac{4}{15}c^2q^2 \times \frac{35}{17} \frac{\omega + \frac{18}{17}z''}{\left(\omega + \frac{18}{17}z''\right)^2 + \left(1/\tau + \frac{18}{17}z'\right)^2}, \quad (8)$$

with z' and z'' defined, respectively, as

$$\begin{aligned} z' &= \text{Re}[\sqrt{c^2q^2 + (i\omega + 1/\tau)^2}] \\ &= \frac{1}{\sqrt{2}} \sqrt{\sqrt{\left(c^2q^2 - \omega^2 + \frac{1}{\tau^2}\right)^2 + \frac{4\omega^2}{\tau^2}} + \left(c^2q^2 - \omega^2 + \frac{1}{\tau^2}\right)}, \\ z'' &= \text{Im}[\sqrt{c^2q^2 + (i\omega + 1/\tau)^2}] \\ &= \text{sign}(\omega) \\ &\quad \times \frac{1}{\sqrt{2}} \sqrt{\sqrt{\left(c^2q^2 - \omega^2 + \frac{1}{\tau^2}\right)^2 + \frac{4\omega^2}{\tau^2}} - \left(c^2q^2 - \omega^2 + \frac{1}{\tau^2}\right)}. \end{aligned}$$

Since the memory function given by Eqs. (7) and (8) effectively contains the infinite hierarchy of the moment equation defined in ET, our spectral formula, Eqs. (5) and (6) armed with Eqs. (7) and (8), can be used regardless of phonon regime, i.e., consistently from hydrodynamic to collisionless regimes.¹³

$S_1(q, \omega)$ corresponds to the thermal light-scattering spectrum if the phonon collisions occur sufficiently frequently (hydrodynamic regime), e.g., at relatively high temperatures.¹³ $S_1(q, \omega)$ is reduced to the thermal Rayleigh spectrum (diffusive central peak with a half width of $D_{\text{th}}q^2$) if $cq\tau_R \gg 1$ or to the second-sound doublet if

$$\tau_R^{-1} < \omega_0 < \tau_N^{-1}, \quad (9)$$

which is the well-known ‘‘window condition.’’^{5,30} On the other hand, $S_2(q, \omega)$ corresponds to the broader central peak due to nonequilibrium viscosity in the phonon gas, and its linewidth is equal to the rate of phonon collisions, viz., $\Gamma_2 = 1/\tau$, in the hydrodynamic regime. However, if τ_R and τ_N become longer such that $cq\tau_R, cq\tau_N > 1$, the linewidths (i.e., line shapes) of both S_1 and S_2 approach each other. All of the above behaviors of the two spectra have been confirmed to

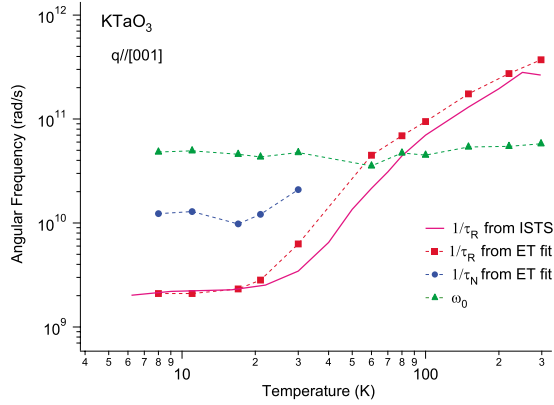


FIG. 5. (Color online) Temperature dependence of τ_R^{-1} (■ and solid line), τ_N^{-1} (●), and ω_0 (▲). The dashed straight lines between the points are guides to the eyes.

be in good agreement with the observations in many crystals.^{21,31–34}

In fitting Eq. (4), we adjusted P_1 , P_2 , C , τ_N , and c as the free parameters. For τ_R , we basically assumed the values estimated from the ISTS measurement of D_{th} but slight adjustment was necessary to achieve better result in the practical fit to the observed spectra. As can be seen in Fig. 4, the fit was reasonably successful for all the temperatures investigated.

From the fit of Eq. (4) to the observed spectra, we have obtained the temperature dependences of τ_N^{-1} , τ_R^{-1} , and ω_0 . The results are shown in Fig. 5. Although τ_R has been slightly adjusted from the values estimated from D_{th} , the deviation of the two results for τ_R^{-1} shown in Fig. 5 is almost within the experimental error in the ISTS measurement. ω_0 is estimated from Eq. (1), substituting the values of c (obtained in the spectral fit) and q . The values of c obtained in the ET fit actually ranged from 1100 to 1800 m/s; this is in reasonable agreement with the average sound velocity we adopted in estimating τ_R from D_{th} , viz., $c=1900$ m/s. Since the fit was not sensitive to τ_N above ~ 30 K, we could obtain the temperature dependence of τ_N only below 30 K. This indicates that the spectral shape is dominated solely by the resistive phonon collisions at higher temperatures. In contrast, this also indicates that τ_N can be determined from the analysis of the low-frequency light-scattering spectra in the low-temperature region while τ_N cannot be measured in other experiments such as in heat-conductivity measurements.³⁵

IV. DISCUSSIONS

Gurevich and Tagantsev³ pointed out that the ferroelectric soft optic-phonon mode, which softens at the Brillouin-zone center, should effectively interacts with the long-wavelength acoustic-phonon modes at low temperature. The phonon collisions between such long-wavelength (i.e., zone-center) phonons allows for the “normal process” in which both energy and quasimomentum of the phonons are conserved. If the “resistive process” in which phonon quasimomentum is not conserved, is less dominant than the normal process, viz., Eq. (9) is satisfied, then propagation of heat, rather than dif-

fusion of heat, is expected. Such a “wave of temperature” is known as the second sound, which offers only a few observations^{18,36} until we reported the likely existence of the second sound in SrTiO_3 recently.^{12,13}

The magnitude of τ_N has been theoretically estimated by Gurevich and Tagantsev³ as

$$\frac{\tau_U}{\tau_N} \approx \sqrt{\epsilon}, \quad (10)$$

where τ_U and ϵ are the umklapp relaxation time and dielectric constant, respectively. The value of ϵ at low temperature was reported²⁶ to be 4200, which gives $\sqrt{\epsilon} \sim 65$. In general, at sufficiently low temperatures, the umklapp collision occurs less frequent than the scattering by impurities or defects, which should effectively dominate the resistive process. Therefore, τ_U^{-1} should be slower than τ_R^{-1} , and we can estimate that $\tau_U/\tau_N \sim 10^{1.8} > \tau_R/\tau_N$, or $\tau_N^{-1} \lesssim 10^{11}$ rad/s; this upper limit of τ_N^{-1} does not contradict our values of τ_N^{-1} shown in Fig. 5. Besides, the numerical calculation by Farhi *et al.*³⁷ has indicated that the width of the acoustic and softened transverse optic-phonon modes at the center of the Brillouin zone are in the range of 10^{10} rad/s, which is also in good agreement with our result.

Figure 5 indicates that the resistive collision becomes less frequent than the second-sound frequency, i.e., $\omega_0\tau_R > 1$, approximately below 60 K. Below 30 K, normal collision is more frequent than the resistive one and the frequency window seems to be open at lower temperatures, i.e., $\tau_R^{-1} < \tau_N^{-1}$. If the second-sound frequency, ω_0 , enters into this frequency range, i.e., Eq. (9) is satisfied, then the propagation of second sound is expected as a “hydrodynamic” collective excitation of phonons.^{5,30} However, it can be seen in Fig. 5 that τ_N^{-1} is always slower than ω_0 , i.e., $\omega_0\tau_N > 1$, at all the temperatures for which τ_N was obtained. That is, the second-sound frequency is “out of the window,” even though the window is open. This is due to the relatively large value of q used in the backscattering experiment; if a q of an order of magnitude smaller is used in the light-scattering experiment, then the doublet spectrum would be sharper and the propagation of the second sound would be expected as in the case of SrTiO_3 (Ref. 12) in which the fulfillment of window condition for the second-sound propagation has been verified. Such a small q value can be realized by setting the scattering angle to be $\sim 10^\circ$ although such small-angle light-scattering experiment is not easy to perform in practice.

To illustrate the phonon regimes in KTaO_3 (Sample 1) for the q value employed in the backscattering experiment, it is convenient to plot the points defined by the “phonon Knudsen numbers” for the resistive and normal processes (Kn_R and Kn_N), which are defined, respectively, as¹³

$$\text{Kn}_R \equiv qc\tau_R \quad \text{and} \quad \text{Kn}_N \equiv qc\tau_N.$$

We show, in Fig. 6, the temperature variation in the points (Kn_R, Kn_N) in KTaO_3 determined in this work, and those in SrTiO_3 determined in our previous work.¹³ In Fig. 6, the upper right area, where both Kn_R and Kn_N are greater than 1, corresponds to the ballistic phonon regime. Since all the points for KTaO_3 plotted in Fig. 6 are in the “ballistic area,”

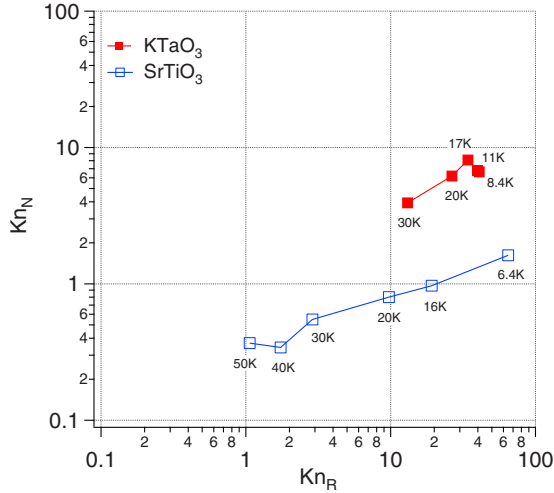


FIG. 6. (Color online) The temperature variation in the phonon Knudsen numbers in KTaO₃. The coordinate of each plotted points is (Kn_R, Kn_N) at each temperature.

the origin of the broad doublet spectrum observed in KTaO₃ is not the well-defined second sound, which postulates many normal phonon collisions and rare resistive collisions, viz., $Kn_N \ll 1 \ll Kn_R$.³⁸ In contrast, the points for SrTiO₃ plotted in Fig. 5 are all in the “second-sound area” except for the 6.4 K point.

A qualitative remark can be made concerning why the normal process in SrTiO₃ is more dominant than in KTaO₃. It is well known^{39–41} that SrTiO₃ undergoes a cubic-to-tetragonal (antiferrodistortive) structural phase transition at around 105 K. Since this phase transition is driven by the freezing of the zone boundary optical-phonon mode (R point, Γ_{25}), the lattice unit cell is doubled and the Brillouin zone is halved, i.e., the zone boundary in the high- T (cubic) phase becomes the zone center in the low- T (tetragonal) phase. The new zone-center optical phonons⁴⁰ in the low- T phase should make an additional contribution to the normal scattering against the acoustic and/or soft optic (ferroelectric, Γ_{15}) modes, in addition to the normal scattering between the acoustic mode and Γ_{15} optic mode; in KTaO₃, only the latter mechanism contributes to the enhancement of the normal scattering.

For the ballistic phonon regime, a hydrodynamic excitation such as the wave of temperature cannot be defined within the length scale of q^{-1} because the phonon gas is considered to be too rarefied for that length scale. In the extreme limit of ballistic regime, the quasielastic light scattering or broad doublet may be viewed as arising due to the second-order Raman processes involving pairs of phonons (two-phonon difference scattering)^{22,42,43} instead of due to well-defined excitation of a collection of phonons. Farhi *et al.*^{15,16,37,44} investigated the broad doublet spectrum in KTaO₃, and they reported that the directional dependence of the emergence of the doublet spectrum implied the two-phonon difference scattering, rather than the second sound, as the origin of the broad doublet. In their analysis, the main

contribution to the line shape was the anisotropy of the phonon dispersions (i.e., anisotropy of the group velocity of phonons), in particular, they found that the strong anisotropy of a TA mode was responsible for the doubletlike line shape. While their numerical calculation of the light-scattering spectrum qualitatively accounted for the observed directional variation in the broad doublet, the calculated line shape was far from quantitative agreement with the observed spectra. The quantitative disagreement may be attributed to their complete neglect of the resistive process and/or to the oversimplification of adopting “pure” two-phonon difference light-scattering process. Strictly speaking, the two-phonon difference light scattering is allowed only in the extreme limit of ballistic regime, and therefore, it can be too crude an approximation for the intermediate regime between the hydrodynamic and ballistic regimes. In contrast, our analysis can be carried out in *any* phonon regime, even if the pure two-phonon difference scattering cannot be considered. Indeed, our spectral formula was successfully fitted to the observed spectra with the finite value of τ_R and the nearly equal value of τ_N to that assumed in the calculation by Farhi *et al.*,¹⁵ i.e., the experimental spectra can be quantitatively reproduced within our model. Our analysis basing on the “isotropic” phonon-gas model¹³ is, of course, not capable of reproducing the directional variation in the spectra without assuming directional dependences of relaxation times and/or average phonon velocities; for more rigorous treatment, a three-dimensional analysis must be carried out. We have shown that our ET analysis becomes equivalent to the two-phonon difference model in the extreme limit of ballistic regime.¹³ Therefore, it is probable that the anisotropy of the broad doublet originates from the anisotropy of the phonon group velocity and/or from the anisotropy of the phonon linewidth as implied by the two-phonon difference analysis by Farhi *et al.* However, as we have shown by the ET analysis, the population of phonons at low temperatures is not small enough for the *pure* two-phonon difference scattering to be considered, i.e., the phonon regime, in which the broad doublet appears, should be considered to be midway between the ballistic and hydrodynamic regimes.

Considering the above mentioned, we can conclude that the broad doublet, which has been observed in KTaO₃ by large angle light scattering with visible light sources, arises from the not well-defined second sound. It should be possible to observe a better defined second sound if a scattering angle as small as 10° is used.

V. SUMMARY

To summarize, we observed the light-scattering spectra in KTaO₃ in the low-frequency region, $\nu \lesssim 100$ GHz. For the entire temperature region investigated, the spectral formula derived from extended thermodynamics was applied for the analysis in any phonon regime, i.e., consistently from the hydrodynamic regime to the ballistic regime. The obtained temperature dependences of τ_N^{-1} and τ_R^{-1} showed that, as was predicted theoretically,³ the rate of the normal scattering of phonons was faster than that of the resistive scattering, and the frequency window for the underdamped second sound

was actually defined below 30 K. However, we found that both the normal and resistive collision frequencies were slightly lower than the second-sound frequency at temperatures approximately below 60 K. This means that the phonon gas in KTaO_3 was too rarefied for the employed light-scattering geometry, viz., $q=5.56 \times 10^7 \text{ m}^{-1}$, to define a well equilibrated collective phonon excitation, such as the second sound or diffusion of heat, within the observation length scale. While the broad-doublet spectrum did appear approximately below 20 K, we concluded that its origin was not the well-defined second sound as in the case of SrTiO_3 , where the window condition for the second-sound propagation was fulfilled around $\sim 30 \text{ K}$.^{12,13} Since the temperature region below 60 K corresponds to the midway between ballistic and hydrodynamic regimes, the spectrum observed in this temperature range should be considered as arising due to the

nonequilibrium light-scattering process. However, the two-phonon difference Raman scattering in its purest form was found to be not suitable in this case because the phonon regime was not purely ballistic. Since our results showed that the frequency window was open, i.e., $\tau_{\text{R}}^{-1} < \tau_{\text{N}}^{-1}$, it should be possible to observe a better defined second sound if an order of magnitude smaller q is employed in a light-scattering experiment. Also, generation of such a temperature wave should be possible by the forced light scattering technique,^{20,45} which is now in progress.

ACKNOWLEDGMENTS

This research was partially supported by the Japan Ministry of Education, Science, Sports and Culture, Grant-in-Aid for Young Scientists B (for A.K.), Grant No. 21740218.

- ¹J. H. Barrett, *Phys. Rev.* **86**, 118 (1952); K. A. Müller and H. Burkard, *Phys. Rev. B* **19**, 3593 (1979).
- ²J. D. Axe, J. Harada, and G. Shirane, *Phys. Rev. B* **1**, 1227 (1970).
- ³V. L. Gurevich and A. K. Tagantsev, *Sov. Phys. JETP* **67**, 206 (1988).
- ⁴B. Hehlen, A.-L. Pérou, E. Courtens, and R. Vacher, *Phys. Rev. Lett.* **75**, 2416 (1995).
- ⁵N. W. Ashcroft and N. Mermin, *Solid State Physics* (Thomson Learning, London, 1976).
- ⁶C. Kittel, *Quantum Theory of Solids* (Wiley, New York, 1963).
- ⁷J. Scott and H. Ledbetter, *Z. Phys. B: Condens. Matter* **104**, 635 (1997).
- ⁸J. F. Scott, A. Chen, and H. Ledbetter, *J. Phys. Chem. Solids* **61**, 185 (2000).
- ⁹M. Yamaguchi, T. Yagi, Y. Tsujimi, H. Hasebe, R. Wang, and M. Itoh, *Phys. Rev. B* **65**, 172102 (2002).
- ¹⁰M. Tan, Y. Tsujimi, and T. Yagi, *J. Korean Phys. Soc.* **46**, 97 (2005).
- ¹¹Y. Tsujimi and M. Itoh, *Ferroelectrics* **355**, 61 (2007).
- ¹²A. Koreeda, R. Takano, and S. Saikan, *Phys. Rev. Lett.* **99**, 265502 (2007).
- ¹³A. Koreeda, R. Takanao, and S. Saikan, *Phys. Rev. B* **80**, 165104 (2009).
- ¹⁴E. Courtens, *Ferroelectrics* **183**, 25 (1996).
- ¹⁵E. Farhi, A. K. Tagantsev, B. Hehlen, R. Currat, L. A. Boatner, and E. Courtens, *Physica B* **276-278**, 274 (2000).
- ¹⁶E. Farhi, A. Tagantsev, B. Hehlen, R. Currat, L. A. Boatner, and E. Courtens, *Ferroelectrics* **239**, 25 (2000).
- ¹⁷J. Callaway, *Phys. Rev.* **113**, 1046 (1959).
- ¹⁸C. C. Ackerman and W. C. Overton, *Phys. Rev. Lett.* **22**, 764 (1969); H. E. Jackson, C. T. Walker, and T. F. McNelly, *ibid.* **25**, 26 (1970).
- ¹⁹R. K. Wehner and R. Klein, *Physica (Utrecht)* **62**, 161 (1972).
- ²⁰K. A. Nelson, R. J. D. Miller, D. R. Lutz, and M. D. Fayer, *J. Appl. Phys.* **53**, 1144 (1982).
- ²¹A. Koreeda, T. Nagano, S. Ohno, and S. Saikan, *Phys. Rev. B* **73**, 024303 (2006).
- ²²K. B. Lyons and P. A. Fleury, *Phys. Rev. Lett.* **37**, 161 (1976).
- ²³E. Courtens, B. Hehlen, G. Coddens, and B. Hennion, *Physica B* **219-220**, 577 (1996).
- ²⁴M. Tachibana, T. Kolodiaznyi, and E. Takayama-Muromachi, *Appl. Phys. Lett.* **93**, 092902 (2008).
- ²⁵G. K. White and S. J. Collocott, *J. Phys. C* **20**, L813 (1987).
- ²⁶B. Salce, J. L. Graviil, and L. A. Boatner, *J. Phys.: Condens. Matter* **6**, 4077 (1994).
- ²⁷D. Jou, J. Casas-Vázquez, and G. Lebon, *Extended Irreversible Thermodynamics*, 3rd ed. (Springer, Berlin, 2001).
- ²⁸W. Dreyer and H. Struchtrup, *Continuum Mech. Thermodyn.* **5**, 3 (1993).
- ²⁹It may be worth noting that, in hydrodynamic regime (i.e., for sufficiently short τ), γ_3 can be further approximated to be simply $\frac{4}{15}c^2q^2\tau$, which can be used to derive the thermal diffusivity or the frequency and linewidth of second sound (Refs. 12 and 13).
- ³⁰R. A. Guyer and J. A. Krumhansl, *Phys. Rev.* **148**, 778 (1966).
- ³¹J. R. Sandercock, *Solid State Commun.* **26**, 547 (1978).
- ³²H. E. Jackson, R. T. Harley, S. M. Lindsay, and M. W. Anderson, *Phys. Rev. Lett.* **54**, 459 (1985).
- ³³P. R. Stoddart and J. D. Comins, *Phys. Rev. B* **62**, 15383 (2000).
- ³⁴A. Koreeda, M. Yoshizawa, S. Saikan, and M. Grimsditch, *Phys. Rev. B* **60**, 12730 (1999).
- ³⁵H. H. Barrett, *Phys. Rev.* **178**, 743 (1969).
- ³⁶C. C. Ackerman, B. Bertman, H. A. Fairbank, and R. A. Guyer, *Phys. Rev. Lett.* **16**, 789 (1966); V. Narayanamurti and R. C. Dynes, *ibid.* **28**, 1461 (1972).
- ³⁷E. Farhi, Ph.D. thesis, Université Montpellier II, 1998.
- ³⁸This is the window condition for second-sound propagation in terms of the phonon Knudsen number (Ref. 13).
- ³⁹H. Unoki and T. Sakudo, *J. Phys. Soc. Jpn.* **23**, 546 (1967).
- ⁴⁰P. A. Fleury, J. F. Scott, and J. M. Worlock, *Phys. Rev. Lett.* **21**, 16 (1968).
- ⁴¹G. Shirane and Y. Yamada, *Phys. Rev.* **177**, 858 (1969).
- ⁴²P. A. Fleury and K. B. Lyons, *Light Scattering Near Phase Transitions* (North-Holland, Amsterdam, 1983), Chap. 7.
- ⁴³R. Klein, *Nonequilibrium Phonon Dynamics* (Plenum, New York, 1985).
- ⁴⁴E. Farhi, A. K. Tagantsev, R. Currat, B. Hehlen, E. Courtens, and L. A. Boatner, *Eur. Phys. J. B* **15**, 615 (2000).
- ⁴⁵D. W. Pohl, S. E. Schwarz, and V. Irniger, *Phys. Rev. Lett.* **31**, 32 (1973).